Physics and Imaging in Radiation Oncology 34 (2025) 100758

Contents lists available at ScienceDirect

Physics and Imaging in Radiation Oncology

journal homepage: www.sciencedirect.com/journal/physics-and-imaging-in-radiation-oncology

Original Research Article

Ultra-low field magnetic resonance breast imaging in prone and seated positions for radiation therapy☆

Friderike K. Longarino [a,b,c,d,1,*], Sheng Shen [e,f,1], Neha Koonjoo [e,f], Torben P.P. Hornung [a,e,g], Rachel B. Jimenez [a,f], Elie K. Mehanna [a], John T. Burge [a], Zoelle Wilson [a], Kathryn E. Keenan [h], Thomas R. Bortfeld [a,f], Matthew S. Rosen [e,f,2], Susu Yan [a,f,2]

[a] Department of Radiation Oncology, Massachusetts General Hospital, Boston, USA
[b] Clinical Cooperation Unit Translational Radiation Oncology, German Cancer Research Center (DKFZ), Heidelberg, Germany
[c] Department of Radiation Oncology, Heidelberg University Hospital, Heidelberg, Germany
[d] Heidelberg Institute for Radiation Oncology (HIRO), National Center for Radiation Research in Oncology (NCRO), Heidelberg, Germany
[e] Athinoula A. Martinos Center for Biomedical Imaging, Charlestown, USA
[f] Harvard Medical School, Boston, USA
[g] Department of Physics, ETH Zürich, Zürich, Switzerland
[h] National Institute of Standards and Technology, Boulder, USA

ARTICLE INFO

Keywords:
Ultra-low field breast MRI
Breast proton therapy
Upright proton therapy
Democratizing proton therapy

ABSTRACT

Background & purpose: The aim of this first-in-human study was to investigate the potential of ultra-low field (ULF) magnetic resonance imaging (MRI) at 6.5 mT for breast imaging in healthy female participants in prone and seated positions for radiation therapy, especially compact proton therapy systems.
Materials & methods: An experimental setup for breast imaging in prone and seated positions utilizing an ULF MRI scanner and a conical RF coil was developed. ULF MR images of the left breast of ten healthy women were acquired in prone and seated positions using a 3D balanced steady-state free precession sequence without the use of contrast agents. The visibility of the breast outline, chest wall, and cardiac silhouette in prone and seated position ULF breast MR images was evaluated by two radiation oncologists (ROs) and two radiation therapists (RTTs), respectively.
Results: ULF breast MRI obtained at 6.5 mT can show breast outline, chest wall, and cardiac silhouette in prone and seated positions. ULF prone/seated images were found to be acceptable by the ROs (RTTs) for treatment planning (setup) purposes in 100%/95% (95%/85%) of cases for breast outline visibility, in 70%/50% (75%/70%) of cases for chest wall visibility, and in 65%/65% (0%/10%) of cases for cardiac silhouette visibility.
Conclusions: This proof-of-concept study demonstrated that breast imaging is feasible in prone and seated positions utilizing ULF MRI and partially suitable for treatment planning and setup in proton therapy. Yet an increased spatio-temporal resolution is required for applications to MRI-guided proton therapy. ULF MRI may enable position monitoring and adaptive treatment procedures in radiation therapy.

1. Introduction

Proton therapy is one of the most precise and advanced forms of radiotherapy due to the favorable energy deposition of charged particles [1]. The availability of and demand for proton therapy is growing exponentially [2]. Yet the long-term projected availability of such therapy is still very limited because of the high cost and large size of the equipment [2,3]. Less than 1 % of radiation therapy patients receive proton therapy [4], although it is believed that between 15 % and 50 % would benefit from it [3]. For certain disease sites, this number may be even higher [2].

A proton therapy system without a gantry could reduce capital costs

☆ This article is part of a special issue entitled: 'Physics highlights from ESTRO 2024' published in Physics and Imaging in Radiation Oncology.

* Corresponding author.
E-mail address: f.longarino@dkfz-heidelberg.de (F.K. Longarino).

[1] These authors contributed equally to this work and share first authorship.
[2] These authors contributed equally to this work and share last authorship.

https://doi.org/10.1016/j.phro.2025.100758
Received 25 October 2024; Received in revised form 22 March 2025; Accepted 24 March 2025
Available online 26 March 2025

and space requirements by having the patient rotate in front of a horizontally fixed proton beamline [2,5,6,7]. Such compact proton therapy systems could increase global accessibility to proton therapy treatment [8]. In such settings, the patient is placed in a seated or reclined position in addition to the current lying position. It is especially crucial to monitor the position of the tumor and organs-at-risk (OARs) before and during treatment to enhance precise dose delivery for proton therapy on such a system [9].

Magnetic resonance imaging (MRI)-guided radiotherapy provides high soft tissue contrast, enables functional imaging, and adds no additional radiation dose to patients [10]. Recent studies have shown that rapid MRI scans can be used for real-time imaging and online adaptive radiotherapy in photon-based radiotherapy systems [11]. Furthermore, low-field MRI has recently shown its fitting application in clinical settings [12,13]; for example, a portable bedside scanner is used in neurology [14,15]. Combining ultra-low field (ULF) MRI ($\leq$ 0.01 T) with proton or photon therapy may offer several advantages. ULF MRI costs significantly less than other techniques, it has submillimeter-level total Bragg peak deflection for an in-beam combination [16], it can be designed in a portable manner [13], it is easy to maintain, it is safe to

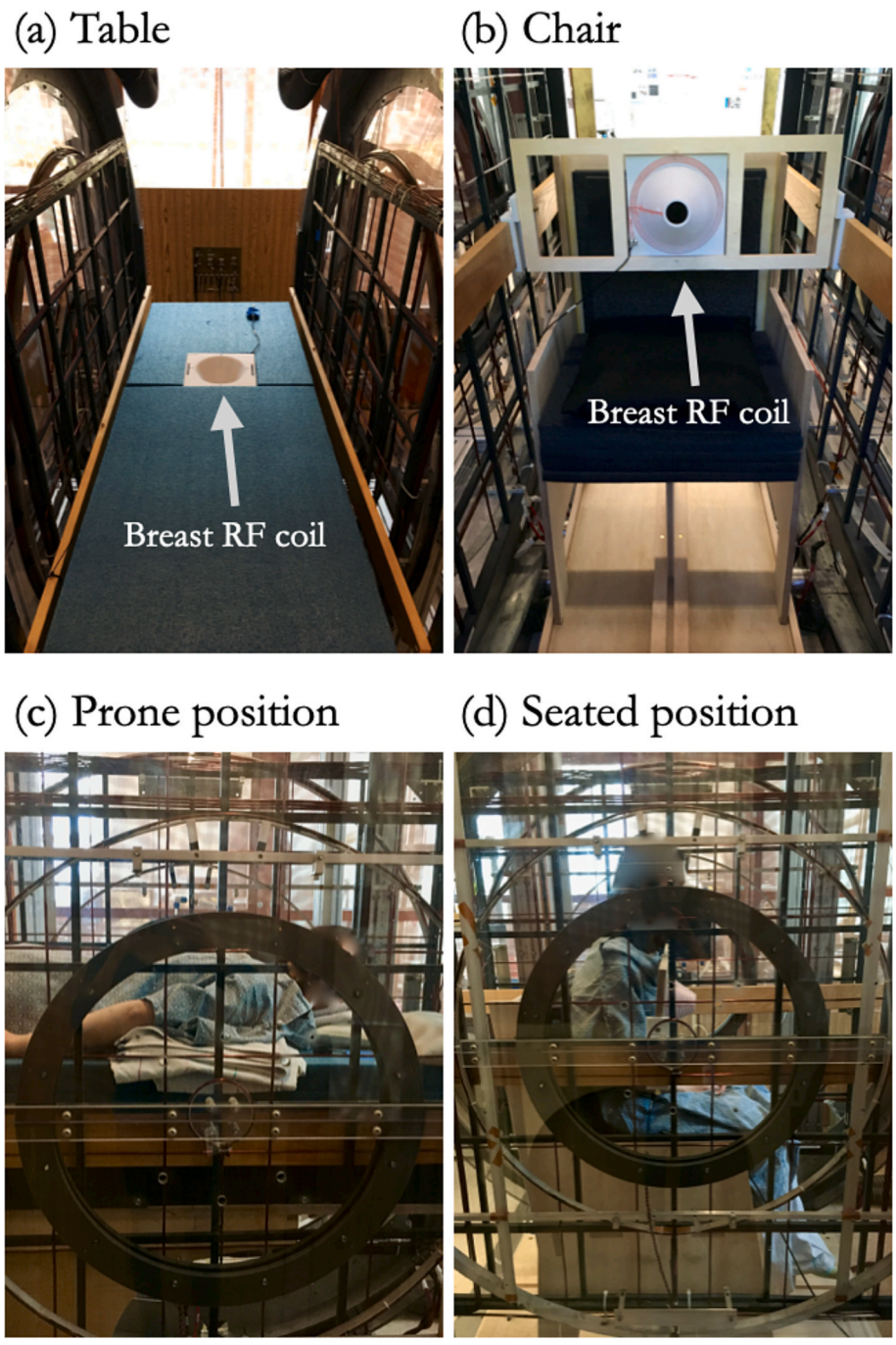

Fig. 1. Experimental setup for single left breast imaging using an ultra-low field (ULF) MRI scanner at 6.5 mT. (a) ULF MRI B_0 coils of the resistive electromagnet are shown on each side of the table with an open design. A wooden table was positioned at the center of the scanner for imaging in the prone position. The gray arrow indicates the transmit/receive radiofrequency (RF) coil, which is embedded in the table. (b) A wooden chair was designed to fit inside the magnet for imaging in the seated position. A single breast RF coil is attached to the wooden frame (gray arrow). A volunteer is shown from the side view in the prone (c) and seated (d) positions.

operate [17], and it also enables imaging in environments where high magnetic fields would be contraindicated. The ULF MRI scanner used in this study features an open design, allowing it to be combined with a horizontal fixed proton or photon beamline in various configurations, such as in-beam, in-room, or near-room setups. In this specific study, the ULF MRI scanner is situated in a stand-alone research lab; the integration of radiation beams for in-beam or in-room configurations will be explored in future studies.

However, as of yet, no study has investigated employing ULF MRI for imaging in different patient orientations that facilitate a horizontal proton or photon beamline treatment. Breast tumors may be one of the disease sites that can be treated with protons while the patient is in a seated position [18]. Treating breast cancer patients in an upright position may better spare the lungs and other OARs [19,20,21], may be easier to set up, and may increase comfort as compared to supine treatments [18,22]. Furthermore, proton therapy has been shown to offer improvements in OARs sparing compared to photon volumetric modulated arc therapy for treating left-sided breast cancer [23].

The aim of this study was to investigate the potential of ULF MRI for breast imaging in healthy female participants in prone and seated positions and to conduct an analysis of the attainable image quality.

2. Material and methods

2.1. Ultra-low field MRI acquisition

The ultra-low field MRI scanner is a custom-built electromagnetic 6.5 mT system with a Larmor frequency of 276 kHz [12] (Fig. 1(a)). The shimmed magnetic field inhomogeneity is less than 10 Hz within a 20 cm diameter spherical region at the isocenter. Magnetic field gradients are generated by a biplanar gradient set capable of producing linear gradients of up to 1 mT/m in all three axes. The open design of the ULF MRI scanner enables imaging in prone and seated positions. The imaging was conducted using a 3D balanced steady-state free precession (bSSFP) sequence with an under-sampling rate of 70 %, a flip angle of 70°, 50 averages, a matrix of 64 × 72 × 21, and a spatial resolution of (3 × 3 × 8) mm^3 in the axial orientation. The repetition time was 26 ms, and the echo time was 13 ms. The acquisition time was 21 min and 36 s (per position and volunteer). The images were reconstructed using inverse fast Fourier transform in MATLAB (MathWorks, Natick, USA), with the under-sampled region zero-filled in k-space. No machine learning was performed.

The study was performed using a single-breast, conical, close-fitting, single-channel radiofrequency (RF) coil. The RF coil was developed in-house by winding multistrand Litz wire on a 3D-printed polycarbonate-based former [16,24]. As the sensitivity of the RF coil decreases from the breast nipple to the chest wall, a signal magnitude modification was performed by scaling the signal according to the computed sensitivity profile of the RF coil from the nipple to the chest wall.

2.2. Experimental setup for imaging in prone and seated positions

A table and chair, both developed in-house and made of wood, were used for imaging in prone and seated positions (Fig. 1(a) and (b)). The table was modified from the brain imaging setup previously described [12]. The chair was designed to fit accurately into the ULF MRI scanner; designs were completed using computer-aided design (CAD) software application (Fusion 360, Autodesk, San Francisco, USA) and computer numerical control (CNC) routing.

For imaging in the prone position (Fig. 1(c)), the breast coil was fitted into the foam and aligned at isocenter using a laser system to ensure it was positioned in the region of most homogeneous B_0. The subject lay down on the table covered with foam pillows, with the left breast enclosed by the breast coil.

For imaging in the seated position (Fig. 1(d)), the subject sat on the chair covered with foam pillows and positioned her left breast into the coil. The breast coil was fitted into a wooden support system that was built in-house, mounted upright to the sides of the scanner, and positioned centrally using a laser system. The height and position of each participant were individually adjusted to minimize slouching and ensure that the breast coil was always positioned at isocenter. Additionally, the angle of the breast coil was adjusted for each participant based on comfort in the seated position.

The aforementioned bSSFP ULF MR imaging was conducted on the volunteers in prone and seated positions without the use of a contrast agent. The volunteers could breathe freely, and no breathing commands were given.

2.3. Study participants

Institutional review board approval from the Office for Human Research Studies (protocol 21–579) at the Dana-Farber/Harvard Cancer Center was obtained. Ten healthy female volunteers (mean age 35 years; range from 21 years to 65 years) were enrolled. Written informed consent was obtained from each participant prior to MRI examination.

2.4. Analysis of the ultra-low field breast MR images

The visibility of the breast outline, chest wall, and cardiac silhouette in the prone and seated position images of all study participants was evaluated by two radiation oncologists (ROs) and two radiation therapists (RTTs), respectively. The ROs reviewed the images to assess their suitability for treatment planning, and the RTTs reviewed the images for setup purposes in proton therapy, each using a 3-point Likert scale (1 – unsuitable for treatment planning/setup, 2 – useable, but suboptimal for treatment planning/setup, 3 – suitable for treatment planning/setup).

Signal-to-noise ratio (SNR) was calculated by dividing the mean signal amplitude in a region of interest in the breast tissue by the standard deviation of the noise in a region considered as background (i.e., edge of the image opposite the body) [16]. Breast tissue was segmented by adjusting the window. The SNR was measured for the central slices of the breast tissue signal, and the mean SNR was calculated for each subject. Furthermore, the study quantified the antero-posterior length of the breast (i.e., chest wall-to-nipple distance) and the imaging depth into the chest wall for all volunteers in prone and seated positions. Additionally, the breast volume was measured and compared in both positions for all volunteers.

3. Results

All enrolled women tolerated the ULF MR imaging well in prone and seated positions. Subject motion did not degrade any of the images. The acquired images covered the left breast in the axial plane, extending from the midsternal line over the midclavicular line to the anterior axillary line (Fig. 2).

ULF breast MRI can show breast outline, chest wall, and cardiac silhouette in both positions (Fig. 2). Table 1 tabulates the ROs' and RTTs' 3-point Likert scale scores. Table 2 illustrates the percentage scores for the three structures in the prone and seated positions, with a view to facilitating treatment planning and setup in proton therapy. The ULF prone/seated breast images were found to be acceptable (i.e., scores $\geq$ 2) by the two evaluating ROs (RTTs) for treatment planning (setup) purposes in 100 %/95 % (95 %/85 %) of cases for breast outline visibility, in 70 %/50 % (75 %/70 %) of cases for chest wall visibility, and in 65 %/65 % (0 %/10 %) of cases for cardiac silhouette visibility.

The mean SNR in the breast tissue across all subjects was 144 ± 28 in the prone position and 126 ± 20 in the seated position. The mean length of the breast was (5.3 ± 1.4) cm in the prone position and (4.4 ± 1.2) cm in the seated position across all volunteers. The mean imaging depth into the chest wall was (4.0 ± 0.7) cm in the prone position and (3.8 ± 0.4) cm in the seated position. The mean breast volume was (532 ± 266) cm^3

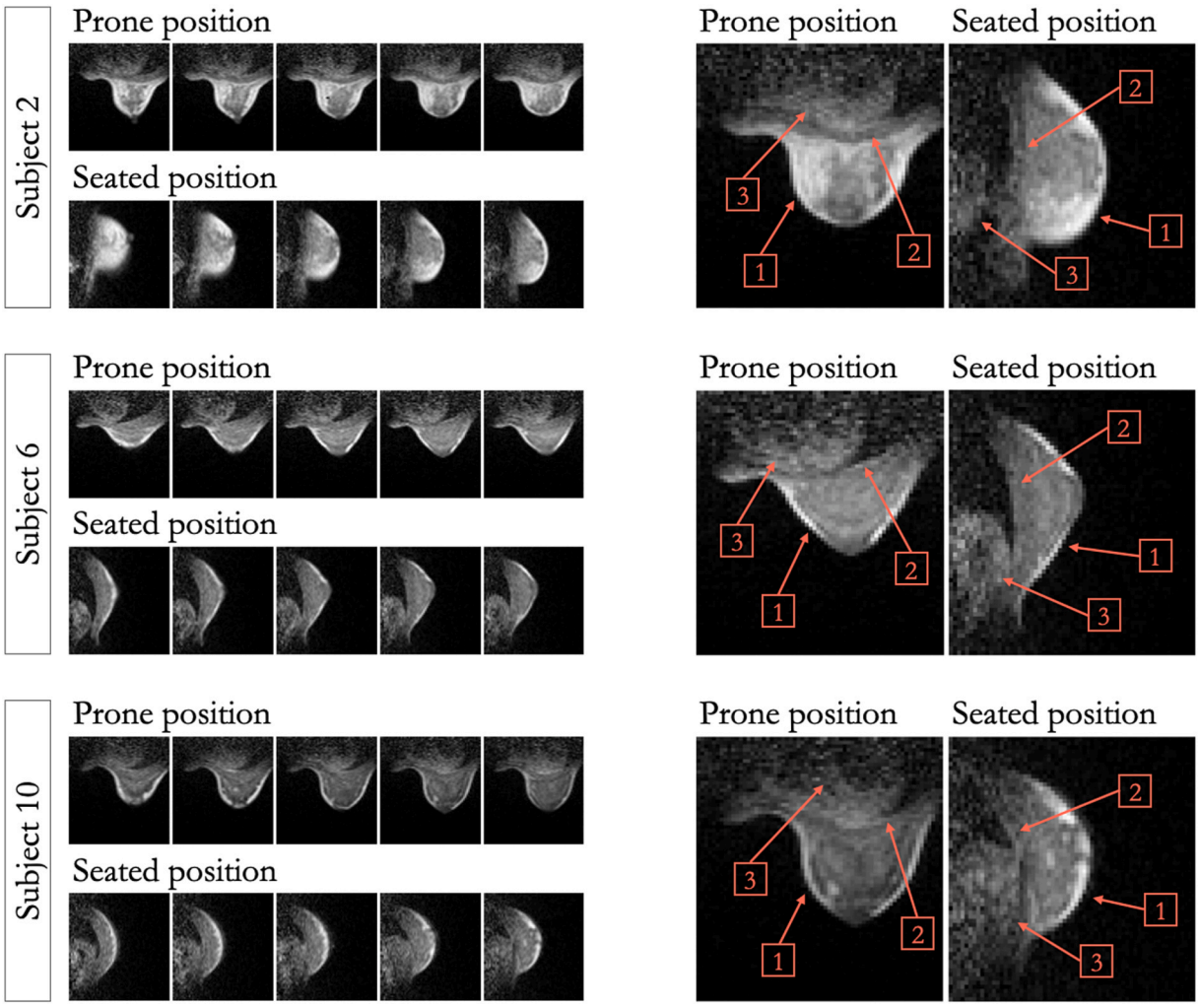

Fig. 2. Ultra-low field (ULF) breast MRI acquired in the prone and seated position with a spatial resolution of ($3 \times 3 \times 8$) mm^3. Image acquisition was performed using a 3D bSSFP imaging sequence, leading to an image contrast that was weighted by the ratio of T_2/T_1. At ULF, the T_1 and T_2 values are typically similar, resulting in mainly proton density weighted images. 5 out of 21 axial slices of the left breast of three healthy female volunteers are shown in prone and seated positions. Additionally, a single central slice from the three subjects is depicted, with labels indicating the breast outline (indicated by 1), the chest wall (indicated by 2), and the cardiac silhouette (indicated by 3).

Table 1
Qualitative assessment of ultra-low field breast MRI in prone (P) and seated (S) positions for ten subjects by two radiation oncologists (ROs) for treatment planning (denoted as A and B) and two radiation therapists (RTTs) for setup purposes (denoted as C and D). A 3-point Likert scale was used to evaluate the breast outline, chest wall, and cardiac silhouette in the images for treatment planning and setup in proton therapy (1 – unsuitable for treatment planning/setup, 2 – useable, but suboptimal for treatment planning/setup, 3 – suitable for treatment planning/setup). Additionally, the mean and standard deviation are presented.

Structure	RO/RTT assessment for treatment planning/ setup purposes		Subject #																				Mean ± standard deviation	
			1		2		3		4		5		6		7		8		9		10			
			P	S	P	S	P	S	P	S	P	S	P	S	P	S	P	S	P	S	P	S	P	S
Breast outline visibility	RO	A	3	3	3	3	3	3	3	3	3	3	3	3	3	3	3	3	3	3	3	3	2.95 ±	2.80 ±
		B	3	3	3	3	3	3	3	3	3	2	3	3	2	1	3	3	3	2	3	3	0.22	0.52
	RTT	C	3	3	3	3	3	3	3	3	3	3	3	3	3	3	3	3	3	3	3	3	2.80 ±	2.60 ±
		D	3	3	3	3	3	3	3	2	3	3	2	2	2	1	1	3	3	1	3	1	0.52	0.75
Chest wall visibility	RO	A	2	1	2	1	3	2	2	2	1	1	3	2	2	1	3	2	3	2	2	1	1.90 ±	1.55 ±
		B	1	2	2	2	2	2	2	1	1	1	1	3	1	1	2	2	2	1	1	1	0.72	0.60
	RTT	C	2	2	3	2	2	1	1	1	1	1	1	3	2	1	2	2	2	2	1	1	2.15 ±	2.00 ±
		D	2	2	3	3	3	3	3	3	3	3	3	3	2	1	1	2	3	2	3	2	0.81	0.79
Cardiac silhouette visibility	RO	A	1	1	2	1	3	2	2	2	1	1	3	3	1	1	2	2	3	3	2	2	1.80 ±	1.80 ±
		B	1	2	2	2	2	2	2	2	1	1	2	3	1	1	1	1	2	2	2	2	0.70	0.70
	RTT	C	1	1	1	1	1	1	1	1	1	1	1	2	1	1	1	1	1	2	1	1	1.00 ±	1.10 ±
		D	1	1	1	1	1	1	1	1	1	1	1	1	1	1	1	1	1	1	1	1	0.00	0.31

Table 2
Percentage scores for breast outline, chest wall, and cardiac silhouette visibility in ultra-low field (ULF) breast MRI in prone and seated positions. ULF breast MRI of ten subjects were assessed by two radiation oncologists (ROs) for treatment planning and two radiation therapists (RTTs) for setup purposes. A 3-point Likert scale was used to evaluate the breast outline, chest wall, and cardiac silhouette in the images for treatment planning and setup in proton therapy (1 – unsuitable for treatment planning/setup, 2 – useable, but suboptimal for treatment planning/setup, 3 – suitable for treatment planning/setup).

Structure	RO/RTT assessment for treatment planning/setup purposes	3-point Likert scale	Prone position (%)	Seated position (%)
Breast outline visibility	Treatment planning	1	0	5
		2	5	10
		3	95	85
	Setup	1	5	15
		2	10	10
		3	85	75
Chest wall visibility	Treatment planning	1	30	50
		2	50	45
		3	20	5
	Setup	1	25	30
		2	35	40
		3	40	30
Cardiac silhouette visibility	Treatment planning	1	35	35
		2	50	50
		3	15	15
	Setup	1	100	90
		2	0	10
		3	0	0

in the prone position and (363 ± 261) cm^3 in the seated position.

4. Discussion

The results, along with their significance and implications, can be summarized as follows.

To fully exploit the potential of proton therapy in terms of an efficient target coverage and sparing of OARs, it is essential to integrate improved anatomical imaging at the time of treatment. This study demonstrated that human breast imaging using ULF MRI is feasible in prone and seated positions (Fig. 2). ULF breast MRI can show breast outline, chest wall, and cardiac silhouette in both positions (Table 1). This is an important first step towards integrating an ULF MRI system into a proton therapy system. The combination of ULF MRI and proton therapy may offer the possibility to combine the high soft tissue contrast and potential real-time imaging capabilities of MRI with the superior dose conformity of proton therapy compared to photon radiotherapy [10].

Our study is the first-in-human investigation of ULF MRI of the breast in different positions. This provides valuable data for MR imaging and radiation oncology. Current ULF MRI was found to be partially suitable for use in treatment planning and setup in proton therapy (Table 2). The breast outline received the highest scores from the ROs and RTTs. The results indicated that the perceived utility of cardiac silhouette visibility differed between setup and planning. RTTs were generally stricter, deeming it unsuitable for setup in most cases, whereas ROs considered the same visibility acceptable for planning purposes. In contrast, for the chest wall, ROs were more stringent about its use in treatment planning, while RTTs found the current visibility acceptable for setup in a greater number of cases. This suggests that the same image quality may meet the needs of planning but fall short for setup precision, or vice versa. The current imaging depth, approximately 4 cm, into the chest wall may be sufficient for proton therapy treatment planning and setup. In general, the ULF breast MR images in the prone position resulted in slightly enhanced visualization of the chest wall and the heart compared to the seated position. While the prone images were rated slightly higher overall, no statistically significant differences (paired *t*-test, $p > 0.05$) were observed in the evaluation of the prone and seated position images.

The length of the breast of the subjects agrees with a previous study that reported a mean chest wall-to-nipple distance of 4.0 cm [25]. The ULF MRI-estimated breast volume in this study is also consistent with the findings of a previous study that reported a mean (SD) breast volume measured by MRI of 687 (312) cm^3 [26].

ULF MRI-guided compact proton therapy systems would substantially reduce the cost of proton therapy systems, while achieving the same, or even better, treatment accuracy, yielding a highly significant societal impact by reducing the global burden of cancer [5]. Although still in its nascent stages, integrated ULF MRI in compact proton therapy systems represents a promising new frontier in the technological advancement of cost-effective proton therapy. This approach has potential for fully exploiting the superior ballistic accuracy of proton beams in treating tumor sites with inter- and intra-fractional motion. Nonetheless, a combination of an ULF MRI scanner with upright photon treatment, which has also been in development, could lower the capital cost of the current MRI-guided photon therapy system.

The strengths and limitations of the study can be summarized as follows.

With a relatively simple proof-of-concept design, the study demonstrated the feasibility of ULF breast imaging in prone and seated positions. The participants self-reported finding the test bed and chair system comfortable during the scanning process. With regard to immobilization in the seated position, participants reported feeling tightly but not unpleasantly bound between the chair's backrest and the coil support system. Furthermore, the participants appreciated the low noise level of the scanner in comparison to high-field scanners. They also found the open design of the scanner to be pleasant, which helped to minimize feelings of claustrophobia.

One of the main challenges in implementing ULF MRI is achieving adequate SNR for imaging and sufficient contrast-to-noise ratio for diagnostic differentiation between tissues within a short imaging time. In this study, an ULF MRI scanner with a magnetic field strength approximately 500 times lower and a SNR approximately 10,000 times lower than that at 3 T was used. The results demonstrated that orientation-variable human breast imaging is nevertheless feasible using a 3D bSSFP imaging sequence that is efficient in SNR at ULF and an efficient close-fitting RF coil. With the current experimental setup, distinct anatomical structures in the breast could be identified. A crucial factor in proton therapy is the imaging time, which impacts treatment planning, setup, and adaptive processes. For proton therapy applications, particularly for image guidance, it is crucial to have high spatial and temporal resolution images to accurately identify target structures and OARs. Therefore, to meet the clinical requirements, the spatial and temporal resolution should be improved from the results presented in this proof-of-concept study.

The study has limitations in that there were no reference high-field (1.5 or 3 T) breast MR images of the participants due to the study approval. Therefore, it was not possible to generate comparison data between low-field and high-field MRI, as has been done in a few previous studies [27,28]. Additionally, the study only included healthy volunteers, so investigating the visibility of breast lesions was not possible. However, it is anticipated that ULF MRI will be investigated in breast cancer patients. It is also important to note that the supine position, which is the conventional treatment position in breast radiotherapy, was not investigated in this study due to the lack of access to a supine positioner for the ULF MRI scanner. Furthermore, the currently used breast coil does not allow for a field-of-view that includes the axilla, although RF coils capable of imaging a field-of-view that includes the axilla may be developed in the future. The visibility of the chest wall and cardiac silhouette was not consistently optimal, particularly in participants with larger breasts, due to the inherent limitations of the RF coil imaging depth. This limitation could be addressed in the future by the development of improved coils.

The following are suggestions for further research.

Differences in breast length and breast volume were observed in all subjects between the prone and seated positions. The breast conformed differently to the coil, depending on whether the volunteer was in the seated or prone position; in the prone position, the breast filled the coil more fully. Consequently, this may have led to greater signal in the prone images, which may have resulted in the higher SNR for prone images compared to those acquired in the seated position. In the future, the use of RF coils that are more specifically tailored to one or the other imaging position may result in further improvements in image quality. Further research may also improve the coil geometry and optimize different coil sizes for different breast sizes. Moreover, multichannel RF coils could be developed and optimized for ULF breast MRI [29]. In the future, patients may also wear suitable bras to manage upright inframammary skin folds [18].

The evaluation, conducted using a 3-point Likert scale, revealed differences in the assessment of the three anatomical structures by the ROs and RTTs for two different purposes of using ULF MRI (treatment planning and setup). The differences in the assessments showed that the ULF MR image acquisition sequence and the breast coil could be optimized for different purposes in a future study. Furthermore, there is a lack of experience among the ROs and RTTs, given that this is their initial experience with ULF MR images. With adequate training and more experience in reviewing ULF MR images, the assessments of the anatomical structures could be refined. The assessments could also be validated in a future study with more ROs and RTTs scoring the ULF MR images.

Further research could investigate patient positioning and optimize immobilization. In this study, the participants positioned their arms on their legs or knees when seated or against their bodies in the prone position. However, it is also possible to position the arms on armrests [30] or to position patients with their arms raised, which may help to extend the thorax. Additionally, in a seated position, the angle of the backrest can be optimized to best spare the heart. In the future, a robotic positioning chair with a soft robotic immobilization device could be utilized [30]. Potential breast deformation due to the coil in the seated position needs to be evaluated. If the coil is removed during proton or photon beam delivery, breast deformation caused by the coil should be minimized. For real-time ULF MRI, where the coil remains in place, a simulation study has been conducted to assess the deflection of the proton beam as it passes through the copper wires of the coil [16]. The study found that the proton projected range decreases by 3.2 mm per layer of copper wire for a 150 MeV beam. Additionally, the lateral spread of the proton beam increases by 0.1 mm as the number of wires increases.

To enhance the clinical utility of ULF MRI for proton therapy, it is essential to increase the SNR. Improved SNR can lead to decreased scan time, increased resolution, or both. Another approach to reducing long scan times is to explore deep learning-based methods for image reconstruction. Furthermore, to decrease image acquisition time, it may be sufficient for MRI guidance in proton therapy to acquire only a few slices, such as two orthogonal slices [31].

Although the results presented here were obtained at 6.5 mT, operating at moderately higher magnetic field strengths would substantially increase the achievable resolution and decrease the scan time. For example, increasing the magnetic field by ten times to 65 mT (still low-field) would result in a 32-fold increase in SNR, as SNR is proportional to $B^{3/2}$ [32]. This increase could allow for obtaining images approximately 1000 times faster while maintaining the same SNR. However, in the envisioned hybrid system, the static magnetic field of the MRI system may affect the proton beam, depending on its strength. A future comparison study of ULF MRI to a higher field MRI would be valuable.

Lastly, future studies are needed to explore the integration of ULF MRI with proton or photon therapy, whether in-beam, in-room, or near-room configurations. The in-beam setup could offer real-time imaging advantages. The open design of ULF MRI, as shown in Fig. 1(a), could accommodate a fixed proton or photon beamline inserted through the open section. However, a key challenge is whether there is enough space to rotate the patient to different orientations for optimal treatment planning. The distance between the biplanar coils of the resistive electromagnet of the ULF MRI scanner is 78 cm, while the chair used in this study is 60 cm wide. A previous study reported an upright radiation therapy chair with a seated hip breadth of 63 cm; this hip breadth accommodates 100 % of males and 99.8 % of females in the American population [33]. In this previous study, the diameter to rotate the patient on the chair was 95 cm for a seated treatment position [33]. For the design of a dedicated ULF MRI scanner for radiotherapy, the required seated hip breadth could be used as a reference. However, the distance between the biplanar coils of the resistive electromagnet depends on the design of the chair. If the patient is in a reclined position—depending on the disease site—a larger distance may be necessary, which needs to be considered when designing the MRI system, radiotherapy chair, and treatment protocols. A new design of open ULF magnets with increased space that can also maintain the homogeneity of the magnetic field may be required and warrants further investigation.

Additionally, the interaction between the proton/photon beam and the ULF MRI magnetic field requires careful study. Although simulations have demonstrated only submillimeter deflection of the Bragg peak at a 6.5 mT magnetic field strength [16], the effects on ULF MR image quality in in-beam and in-room configurations still need to be evaluated. Research prototypes of MRI systems operating at 220 mT, integrated with pencil beam scanning proton therapy, have shown ghosting artifacts [34]. While it may not be feasible to bring the current version of the 6.5 mT research MRI scanner from the stand-alone research lab into a proton treatment room, a 64 mT portable MRI scanner for brain imaging [13] is currently being tested to assess the impact of proton beams on MR image quality in an in-room configuration. This future study could reveal the potential of low-field MRI in proton therapy rooms.

Meanwhile, simulation studies will remain of interest until ULF MRI can be fully integrated with proton/photon beamlines to experimentally examine potential interference. For instance, proton deflection has been simulated for magnetic field strengths ranging from 6.5 mT to 500 mT [16], with deflections ranging from submillimeter to 4 mm for 150 MeV protons, and from submillimeter to 10 mm for 200 MeV protons. Further investigation is needed to balance the trade-off between longer scan times and minimal deflection at ultra-low magnetic field strengths, and the use of higher field strengths. Other factors, such as hardware design and economic considerations, also warrant further study.

In summary, ULF MRI has the potential to be used for breast imaging in prone and seated positions for compact proton therapy system settings. With further development and higher spatio-temporal resolution, ULF MRI may be used for position monitoring and for enabling adaptive treatment procedures for tumor sites with inter- and intra-fractional motion.

NIST Disclaimer

Certain commercial equipment, instruments, software or materials are identified in this paper in order to specify the experimental procedure adequately. Such identification is not intended to imply recommendation or endorsement by NIST, nor is it intended to imply that the materials or equipment identified are necessarily the best available for the purpose.

Declaration of competing interest

The authors declare the following financial interests/personal relationships which may be considered as potential competing interests: MSR is a founder and equity holder of Hyperfine, Inc. MSR has a financial interest in DeepSpin GmbH. These interests were reviewed and are managed by Massachusetts General Hospital and Mass General Brigham in accordance with their conflict of interest policies. The other authors declare that they have no known competing financial interests

or personal relationships that could have appeared to influence the work reported in this paper.

Acknowledgments

This work was supported in part by the National Institutes of Health grant 1R21CA267315 (PI Matthew S. Rosen). Matthew S. Rosen acknowledges the generous support of the Kiyomi and Ed Baird MGH Research Scholar award. Friderike K. Longarino gratefully acknowledges support from the German-American Fulbright Commission.

References

[1] Durante M, Flanz J. Charged particle beams to cure cancer: Strengths and challenges. Semin Oncol 2019;46(3):219–25. https://doi.org/10.1053/j.seminoncol.2019.07.007.
[2] Yan S, Ngoma TA, Ngwa W, Bortfeld TR. Global democratisation of proton radiotherapy. Lancet Oncol 2023;24(6):e245–54. https://doi.org/10.1016/S1470-2045(23)00184-5.
[3] Bortfeld TR, Loeffler JS. Three ways to make proton therapy affordable. Nature 2017;549(7673):451–3. https://doi.org/10.1038/549451a.
[4] Mohan R, Grosshans D. Proton therapy - Present and future. Adv Drug Deliv Rev 2017;109:26–44. https://doi.org/10.1016/j.addr.2016.11.006.
[5] Bortfeld TR, Viana MF, Yan S. The societal impact of ion beam therapy. Z Med Phys 2021;31(2):102–4. https://doi.org/10.1016/j.zemedi.2020.06.007.
[6] Paganetti H, Beltran C, Both S, Dong L, Flanz J, Furutani K, et al. Roadmap: proton therapy physics and biology. Phys Med Biol 2021;66(5):05RM01. https://doi.org/10.1088/1361-6560/abcd16.
[7] Schreuder N, Ding X, Li Z. Fixed beamlines can replace gantries for particle therapy. Med Phys 2022;49(4):2097–100. https://doi.org/10.1002/mp.15531.
[8] Volz L, Korte JC, Martire MC, Zhang Y, Hardcastle N, Durante M, et al. Opportunities and challenges of upright patient positioning in radiotherapy. Phys Med Biol 2024;69(18):18TR02. https://doi.org/10.1088/1361-6560/ad70ee.
[9] Yan S, Lu H-M, Flanz J, Adams J, Trofimov A, Bortfeld T. Reassessment of the Necessity of the Proton Gantry: Analysis of Beam Orientations From 4332 Treatments at the Massachusetts General Hospital Proton Center Over the Past 10 Years. Int J Radiat Oncol Biol Phys 2016;95(1):224–33. https://doi.org/10.1016/j.ijrobp.2015.09.033.
[10] Hoffmann A, Oborn B, Moteabbed M, Yan S, Bortfeld T, Knopf A, et al. MR-guided proton therapy: a review and a preview. Radiat Oncol 2020;15:129. https://doi.org/10.1186/s13014-020-01571-x.
[11] Otazo R, Lambin P, Pignol JP, Ladd ME, Schlemmer H-P, Baumann M, et al. MRI-guided radiation therapy: an emerging paradigm in adaptive radiation oncology. Radiology 2021;298(2):248–60. https://doi.org/10.1148/radiol.2020202747.
[12] Sarracanie M, LaPierre CD, Salameh N, Waddington DEJ, Witzel T, Rosen MS. Low-cost high-performance MRI. Sci Rep 2015;5:15177. https://doi.org/10.1038/srep15177.
[13] Kimberly WT, Sorby-Adams AJ, Webb AG, Wu EX, Beekman R, Bowry R, et al. Brain imaging with portable low-field MRI. Nat Rev Bioeng 2023;1:617–30. https://doi.org/10.1038/s44222-023-00086-w.
[14] Mazurek MH, Cahn BA, Yuen MM, Prabhat AM, Chavva IR, Shah JT, et al. Portable, bedside, low-field magnetic resonance imaging for evaluation of intracerebral hemorrhage. Nat Commun 2021;12(1):5119. https://doi.org/10.1038/s41467-021-25441-6.
[15] Yuen MM, Prabhat AM, Mazurek MH, Chavva IR, Crawford A, Cahn BA, et al. Portable, low-field magnetic resonance imaging enables highly accessible and dynamic bedside evaluation of ischemic stroke. Sci Adv 2022;8(16):eabm3952. https://doi.org/10.1126/sciadv.abm3952.
[16] Hornung TPP, Koonjoo N, Shen S, Longarino FK, Keenan KE, Yan S, et al. Breast Coil Optimization for Low Field MRI and future MR-guided Proton Therapy. IEEE Trans Biomed Eng 2025. https://doi.org/10.1109/TBME.2024.3520895.
[17] Arnold TC, Freeman CW, Litt B, Stein JM. Low-field MRI: clinical promise and challenges. J Magn Reson Imaging 2023;57(1):25–44. https://doi.org/10.1002/jmri.28408.
[18] Boisbouvier S, Underwood T, McNamara J, Probst H. Upright patient positioning for gantry-free breast radiotherapy: feasibility tests using a robotic chair and specialised bras. Front Oncol 2023;13:1250678. https://doi.org/10.3389/fonc.2023.1250678.
[19] Yang J, Chu D, Dong L, Court LE. Advantages of simulating thoracic cancer patients in an upright position. Pract Radiat Oncol 2014;4(1):e53–8. https://doi.org/10.1016/j.prro.2013.04.005.
[20] Rahim S, Korte J, Hardcastle N, Hegarty S, Kron T, Everitt S. Upright radiation therapy—a historical reflection and opportunities for future applications. Front Oncol 2020;10:213. https://doi.org/10.3389/fonc.2020.00213.
[21] Marano J, Kissick MW, Underwood TSA, Laub SJ, Lis M, Schreuder AN, et al. Relative thoracic changes from supine to upright patient position: a proton collaborative group study. J Appl Clin Med Phys 2023;24(12):e14129. https://doi.org/10.1002/acm2.14129.
[22] Probst H, Rosbottom K, Crank H, Stanton A, Reed H. The patient experience of radiotherapy for breast cancer: a qualitative investigation as part of the SuPPORT 4 All study. Radiography 2021;27(2):352–9. https://doi.org/10.1016/j.radi.2020.09.011.
[23] Bonaccorsi SG, Tessonnier T, Hoeltgen L, Meixner E, Harrabi S, Hörner-Rieber J, et al. Exploring Helium Ions' potential for post-mastectomy left-sided breast cancer radiotherapy. Cancers (Basel) 2024;16(2):410. https://doi.org/10.3390/cancers16020410.
[24] Shen S, Xu Z, Koonjoo N, Rosen MS. Optimization of a close-fitting volume RF coil for brain imaging at 6.5 mT using linear programming. IEEE Trans Biomed Eng 2021;68(4):1106–14. https://doi.org/10.1109/TBME.2020.3002077.
[25] Brown TP, Ringrose C, Hyland RE, Cole AA, Brotherston TM. A method of assessing female breast morphometry and its clinical application. Br J Plast Surg 1999;52(5):355–9. https://doi.org/10.1054/bjps.1999.3110.
[26] Killaars RC, Preuβ MLG, de Vos NJP, van Berlo CCJLY, Lobbes MBI, van der Hulst RRWJ, et al. Clinical assessment of breast volume: can 3D imaging be the gold standard? Plast Reconstr Surg Glob Open 2020;8(11):e3236. https://doi.org/10.1097/GOX.0000000000003236.
[27] Sittek H, Perlet C, Herrmann K, Linsmeier E, Kolem H, Untch M, et al. MR Imaging of the breast. Localization of focal breast lesions with the magnetom open at 0.2 T. Radiologe 1997;37:685–91. https://doi.org/10.1007/s001170050269.
[28] Pääkkö E, Reinikainen H, Lindholm E-L, Rissanen T. Low-field versus high-field MRI in diagnosing breast disorders. Eur Radiol 2005;15(7):1361–8. https://doi.org/10.1007/s00330-005-2664-6.
[29] Marques JP, Simonis FFJ, Webb AG. Low-field MRI: an MR physics perspective. J Magn Reson Imaging 2019;49(6):1528–42. https://doi.org/10.1002/jmri.26637.
[30] Buchner T, Yan S, Li S, Flanz J, Hueso-González F, Kielty E, et al. A soft robotic device for patient immobilization in sitting and reclined positions for a compact proton therapy system. 8th IEEE RAS/EMBS International Conference for Biomedical Robotics and Biomechatronics BioRob 2020:981–8. https://doi.org/10.1109/BioRob49111.2020.9224389.
[31] Hickey S, Reichert A, Ptacek W, Bielak L, Reiss S, Fischer J, et al. Simultaneous T2-weighted real-time MRI of two orthogonal slices. Magn Reson Med 2023;90(6):2388–99. https://doi.org/10.1002/mrm.29795.
[32] Hoult DI, Richards RE. The signal-to-noise ratio of the nuclear magnetic resonance experiment. J Magn Reson 1976;24(1):71–85. https://doi.org/10.1016/0022-2364(76)90233-X.
[33] Korte JC, Wright M, Krishnan PG, Winterling N, Rahim S, Woodford K, et al. A radiation therapy platform to enable upright cone beam computed tomography and future upright treatment on existing photon therapy machines. Med Phys 2025;52:1133–45. https://doi.org/10.1002/mp.17523.
[34] Gantz S, Hietschold V, Hoffmann AL. Characterization of magnetic interference and image artefacts during simultaneous in-beam MR imaging and proton pencil beam scanning. Phys Med Biol 2020;65(21):215014. https://doi.org/10.1088/1361-6560/abb16f.